2016 International Symposium on Nonlinear Theory and Its Applications,
NOLTA2016, Yugawara, Japan, November 27th-30th, 2016

Simulation of cardiac excitation propagation and the circulatory dynamics

Akira AMANO†, Hiromasa UTAKI†, Kosuke TANIGUCHI† and Yukiko HIMENO†

†Department of Bioinformatics, Ritsumeikan University
1–1–1 Nojihigashi, Kusatsu, Shiga 525-8577, Japan
Email: a-amano@fc.ritsumei.ac.jp

Abstract—In the clinical application, indices of whole body condition is required, on the other hand, detailed genome information often appears in the cutting edge of the basic medical research. To connect these information, we constructed a whole body hemodynamics model which consists of cellular contraction model, whole body blood vessel model and left ventricle model which can evaluate the effect of excitation propagation of left ventricle to the hemodynamics.

1. Introduction

Circulation system consists of heart and blood vessels. Blood vessels consist of artery and vein, and heart has four chambers: left and right atriums and ventricles. Human aortic blood pressure is carefully controlled to be in the physiological range of maximum 120 to 130 [mmHg] and minimum 80 to 85 [mmHg]. Heart pump function is based on the electrical excitation of cardiac cells which starts at pacemaker cells in the right atrium, and after excitation of left and right atrium, left and right ventricles are stimulated. These electrical activities can be observed with electrocardiogram (ECG), which shows 60 - 100 [ms] duration of QRS complex that corresponds to the whole heart activation time.

Since the blood pressure is one of the most important factor which determines the extracellular condition, there are several controlling mechanisms which maintains blood pressure to the physiological range. These control systems have different temporal scales. First mechanism is included in the cardiac cell, which is called force length relationship of the ventricular cell. The ventricular cell is known to have characteristics that the contraction force increases according to the increase of the initial cell length. By this mechanism, if the venous return volume increases, then the blood will be pumped out by the larger pressure. Second mechanism is called baroreflex which is controlled by autonomic nervous system (ANS). There are two blood pressure sensors in the mammalian body, and the sensed pressure information is sent to the ANS. The ANS then sends signal to sympathetic or parasympathetic nervous system and the corresponding neurotransmitter is released to the cardiac cells, which controls heart rate and contraction force. Third mechanism is called renin-angiotensin system which controls total blood volume and vasoconstriction.

These mechanisms are discovered by experiments based on single cell and whole body, i.e. microscopic and macroscopic experimental targets, however, experiments on mesoscopic targets are still not fully discovered since the experiments are often difficult to conduct.

To evaluate the effect of known intercellular interaction on the blood pressure, we used a circulation model incorporating cardiac tissue model.

2. Hemodynamics Model

In this research, we used a human hemodynamic model consists of blood circulation model, an LV geometric model and a cardiac tissue model. The cardiac tissue model was constructed by connecting 10 cardiac cellular contraction models in the fiber direction to incorporate the effect of activation time.

2.1. Circulation Model

A circulation model proposed by Heldt et al. [1] (Heldt model) was used as a whole body circulation model. In our model, the LV compartment was replaced by the LV geometric model. To separate the effects of AT from other factors, the baroreflex model included in the Heldt model was removed. Cardiac cycle length was fixed at 1000 [ms]. In our combined model, we defined preload factor K_{rp} and used this factor to modify venous resistances.

2.2. Cardiac Cell and Tissue Model

We used the cardiac cellular contraction model proposed by Negroni and Lascano (NL08) [2] which offers good reproducibility in isometric and isotonic contraction, and also at various transient length changes, based on the good reproducibility of velocity-dependent stress decrease characteristics.

Cellular contraction stress (F_b [mN/mm^2]) is calculated from the state transition model of the troponin system and mechanical model of the half sarcomere.

Since characteristics of the end-diastolic pressure volume relationship (EDPVR) are similar in rats [3] and humans [4], by linearly scaling the stress axis with the identical half sarcomere length axis, we used the following mammalian exponential function as a human passive elastic stress (F_p [mN/mm^2]) model showing good agreement

Table 1: Determined scale parameter values in the normal human hemodynamic model

L_0 [μm]	D	K_{PE} [mN/mm^2]	K_{PL} [mN/mm^2]	K_S	$F_b(t_{ED})$ [mN/mm^2]	K_{fb}	K_{rp}	K_{ra}
1.043	28.1	0.269	7.56	7.24	$5.33{\cdot}10^{-2}$	22.6	1.67	1.52

Table 2: Parameters in Eq. (3) and (4).

Q_m [μM/ms]	t_1 [ms]	Q_{pump_rest} [μM/ms]	K_p [μM/ms]	K_m [μM]
3.2	8	0.03	0.15	0.2

with the experimental data [5, 6]. The format of this equation was based on the equation used by Shim et al. [7] and Landesberg et al. [8].

$$F_p = \begin{cases} -K_{PL} \cdot (1 - \frac{L}{L_0}) & L < L_0 \\ K_{PE} \cdot \left(e^{D(\frac{L}{L_0} - 1)} - 1 \right) & otherwise \end{cases} \quad (1)$$

Note that L_0 [μm] is resting half sarcomere length. D, K_{PL} [mN/mm^2] and K_{PE} [mN/mm^2] are the scale parameters for the heart wall and cardiac cell passive elasticity. Parameter values were manually obtained to reproduce physiological human hemodynamics (Table 1).

Since F_p is usually measured using a piece of tissue, we can consider that the characteristics of F_p are compatible with the macroscopic properties. On the other hand, since F_b is usually measured with a single cell or small piece of ventricular fiber in which the effective cross-sectional area is difficult to measure, measured stress may contain large scale errors. We thus introduced a scale factor, K_s, which is multiplied only to F_b to adjust cellular contraction stress. Finally, total muscle stress F [mN/mm^2] as used in Eq. (6) as wall stress is calculated as follows.

$$F = K_s \cdot F_b + F_p \quad (2)$$

Stimulation time in the NL08 model is controlled by the Ca^{2+} release equation. The release and uptake of Ca^{2+} by the sarcoplasmic reticulum (Q_{rel} [μM/ms] and Q_{pump} [μM/ms]) in the NL08 model are expressed using the following equations.

$$\begin{aligned} Q_{rel} &= Q_m \cdot (t/t_1)^4 \\ &\quad \cdot e^{4(1-t/t_1)} + Q_{pump\_rest} \quad (3) \\ Q_{pump} &= K_p/(1 + (K_m/[Ca^{2+}])^2) \quad (4) \end{aligned}$$

where t [ms] is the time parameter, $[Ca^{2+}]$ [μM] is the concentration of Ca^{2+}, Q_m [μM/ms] is the maximum level of Ca^{2+} release, t_1 [ms] is the interval to maximum Q_{rel}, Q_{pump_rest} [μM/ms] is a parameter to determine Ca^{2+} at rest, K_p [μM/ms] is maximum value of Q_{pump} and K_m [μM] is the value of $[Ca^{2+}]$ for $Q_{pump} = K_p/2$. Parameter values used in Eq. (3) and (4) are shown in Table 2.

Since the heart can be decomposed into several long fiber bundles, we assumed that one fiber bundle surrounding the LV can be considered as a LV wall tissue model with an AT. We thus used a cardiac tissue model constructed by connecting 10 cardiac cellular contraction models in the fiber direction (10-cell model), which represents a fiber bundle surrounding the LV.

In this model, half sarcomere length was calculated by the average of 10 cells, and total muscle stress was assumed to be the same with 10 cells.

ATs can be altered by modifying the time parameter t in the equation Q_{rel} (Eq. (3)) by a constant time (δ_{delay} [ms]).

Since there are 10 cells in the tissue model, the relationship between AT and δ_{delay} becomes the following.

$$AT = \delta_{delay} \times 9 \quad (5)$$

As mentioned in Section 1, AT is closely related to QRS duration. QRS duration is under 100 [ms] in healthy human adult. On the other hand, under pathological conditions, QRS duration can be longer than 200 [ms] [9]. Here we assumed that LV AT is almost the same as QRS duration and defined two AT conditions by fixing δ_{delay} at 11 [ms] and 23 [ms].

2.3. Left Ventricle Model

In the hemodynamic model, the following geometric model based on Laplace's law was used to relate LV pressure ($p_{lv}(t)$ [mmHg]), radius ($R_{lv}(t)$ [cm]), wall thickness ($h_{lv}(t)$ [mm]) and wall stress ($F(t)$ [mN/mm^2]) [10].

$$\frac{p_{lv}(t)}{h_{lv}(t)} = \frac{1.5 \cdot F(t)}{R_{lv}(t)} \quad (6)$$

Since the primary variables in the hemodynamic model are LV pressure (p_{lv} [mmHg]), volume (V_{lv} [mL]), half sarcomere length (L [μm]) and wall stress (F [mN/mm^2]), we have to provide the relationship between LV radius (R_{lv} [cm]) and V_{lv}, between R_{lv} and L, and between LV wall thickness (h_{lv} [mm]) and F.

We used the following reported data to define mathematical equations for the relationship between R_{lv} and V_{lv}. Corsi et al. [11] measured the time course of human LV volume, and Sutton et al. [12] measured the time course of human LV internal radius. Also, Rodriguez et al. [13] reported the time course of canine LV volume, and Sabbah et al. [14] reported the time course of canine LV diameter. We assumed that the realtion will be represented by the following equation, and from the reported data, we obtained

Table 3: Parameters in LV geometric model.

V_γ [mL]	K_β	K_α	C_L [μm/cm]	L_b [μm]	$F_b(t_{ED})$ [mN/mm^2]	$F_b(t_{ES})$ [mN/mm^2]	$h_{lv}(t_{ED})$ [mm]	$h_{lv}(t_{ES})$ [mm]
35.0	2.33	3.92	0.163	0.782	0.465	8.14	10	17

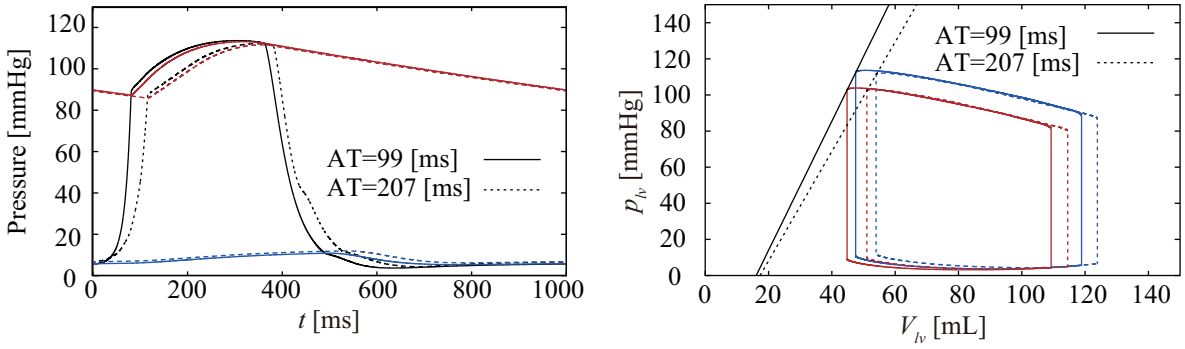

(a) Time courses of p_a, p_v, p_{lv}.

(b) PV loops and ESPVRs.

Figure 1: Time courses of p_a, p_v, p_{lv} and PV loops at different ATs.

$K_\alpha = 3.92$.

$$R_{lv}(t) = \left(\frac{V_{lv}(t) - V_\gamma}{K_\beta}\right)^{1/K_\alpha} \tag{7}$$

Note that $V_{lv}(t)$ [mL] denotes LV volume and the same as V_{lv}. V_γ [mL] is the V_{lv}-intercept of the relationship between V_{lv} and R_{lv}.

We used the following reported data to define mathematical equations for the relationship between R_{lv} and L. Rodriguez et al. [13] also measured the time course of canine sarcomere length. By combining this data with the measured canine time course of internal diameter as reported by Sabbah et al. [14], we obtained a linear relationship between LV diameter R_{lv} and sarcomere length L as $L(t) = C_L \cdot R_{lv}(t) + L_b$.

Next, we considered wall thickness. Yun et al. [15] measured the time course of LV volume, twist angle, and wall thickness, and reported that both volume and twist angle showed relationships with wall thickness. We assumed that cellular contraction stress ($F_b(t)$ [mN/mm^2]) is linearly related to $h_{lv}(t)$.

Parameter values of the LV geometric model are shown in Table 3.

3. Simulation Results

To realize the physiological hemodynamics, we need to adjust parameters included in the model. We have proposed a method to determine these parameter values by using three end-diastolic points and one end-systolic point [16]. By the method, we obtained the scale parameter values shown in Table 1.

Table 4: Hemodynamic parameters and parameters used to represent characteristics of the cell and cardiac cycle obtained at AT= 99 [ms] (normal AT) and 207 [ms] (prolonged AT).

	AT=99 [ms]	AT=207 [ms]
$p_{lv}(t_{ES})$ [mmHg]	112.3	111.1
$p_{lv}(t_{ED})$ [mmHg]	5.81	6.77
$V_{lv}(t_{ES})$ [mL]	47.5	54.0
$V_{lv}(t_{ED})$ [mL]	119	124
$L(t_{ES})$ [μm]	1.0323	1.0604
$L(t_{ED})$ [μm]	1.1886	1.1947
SV [mL]	71.4	69.9
EF [%]	60.0	56.4
peak p_{lv} [mmHg]	113.6	112.1
max dp/dt [mmHg/ms]	6.18	3.48
E_{max} [mmHg/mL]	3.58	3.03

Next, we performed simulation with two different ATs and observed the effects of AT prolongation on LV. Numerical values of hemodynamic parameters and parameters used to represent characteristics of the cell and cardiac cycle obtained from this simulation study are listed in Table 4. Time courses of p_{lv}s for the two different ATs were superimposed on corresponding traces of aortic pressure (p_a) and venous pressure (p_v) in Fig. 1(a). We found that $p_{lv}(t_{ES})$ and $p_{lv}(t_{ED})$ changed by only -1.2 [mmHg] and $+0.96$ [mmHg], respectively. Both $V_{lv}(t_{ES})$

and $V_{lv}(t_{ED})$ were confirmed to increase when AT was prolonged. Since both $V_{lv}(t_{ES})$ and $V_{lv}(t_{ED})$ increased by similar amounts (6.5 [mL] and 5 [mL]), SV did not change markedly. The peak value of p_{lv} was unchanged, whereas max dp/dt showed a large decrease after AT prolongation. Simulation results showed that the isovolumic contraction phase is markedly prolonged and onset time of ejection phases is delayed by AT prolongation, which is supposed to be the outcome of decreased dp/dt.

From the time courses of p_{lv} and V_{lv}, we obtained the PV loops as shown in Fig. 1(b) that have similar properties to the reported human PV loop.

Decrease in max dp/dt was one of the most prominent effects of AT prolongation among all hemodynamic parameters. Decreases in values by changing AT from normal 99 [ms] to prolonged 207 [ms] were small for EF (-6%) and almost negligible (-2%) for SV. The decrease in EF was induced by the larger $V_{lv}(t_{ED})$ at longer ATs.

4. Conclusion

Since the elements of the hemodynamics model are based on the existing models, there are no additional mechanisms to the previously studied hemodynamics model. However, by using the serially connected cardiac cell model as the cardiac tissue model, a new mechanism of maintaining the hemodynamics against the excitation delay was found. Since this finding is based on the simulation model, further investigation with animal experiments will be necessary.

References

[1] Heldt T, Shim EB, Kamm RD, Mark RG: Computational modeling of cardiovascular response to orthostatic stress. J Appl Physiol. **92**(3), pp. 1239-1254, 2002D

[2] Negroni JA, Lascano EC: Simulation of steady state and transient cardiac muscle response experiments with a Huxley-based contraction model. J Mol Cell Cardiol. **45**(2), pp. 300-312, 2008.

[3] Klotz S, Hay I, Zhang G, Maurer M, Wang J, Burkoff D: Development of heart failure in chronic hypertensive Dahl rats focus on heart failure with preserved ejection fraction. Hypertension. **47**(5), pp. 901-911, 2006D

[4] Corin WJ, Murakami T, Monrad ES, Hess OM, Krayenbuehl HP: Left ventricular passive diastolic properties in chronic mitral regurgitation. Circulation. **83**(3), pp. 797-807, 1991D

[5] de Tombe PP, Ter Keurs HE: An internal viscous element limits unloaded velocity of sarcomere shortening in rat myocardium. J Physiol. **454**(1), pp. 619-642, 1992D

[6] Granzier HL, Irving TC: Passive tension in cardiac muscle: contribution of collagen, titin, microtubules, and intermediate filaments. Biophys J. **68**(3), pp. 1027-1044, 1995D

[7] Shim EB, Amano A, Takahata T, Shimayoshi T, Noma A: The cross-bridge dynamics during ventricular contraction predicted by coupling the cardiac cell model with a circulation model. J Physiol Sci. **57**(5), pp. 275-285, 2007D

[8] Landesberg A, Sideman S: Mechanical regulation of cardiac muscle by coupling calcium kinetics with cross-bridge cycling: a dynamic model. Am J Physiol Heart Circ Physiol. **267**(2), pp. 779-795, 1994D

[9] Barold SS, Mugica J: The Fifth Decade of Cardiac Pacing, 1st ed. Wiley-Blackwell, 2003.

[10] Thomas F, Moriarty: The law of Laplace. Its limitations as a relation for diastolic pressure, volume, or wall stress of the left ventricle. Circ Res. **46**(3), pp. 321-331, 1980D

[11] Corsi C, Veronesi F, Lamberti C, Bardo DME, Jamison EB, Lang RM, Mor-Avi V: Automated frame-by-frame endocardial border detection from cardiac magnetic resonance images for quantitative assessment of left ventricular function: validation and clinical feasibility. J Magn Reson Im. **29**(3), pp. 560-568, 2009D

[12] Sutton MG, Tajik AJ, Gibson DG, Brown DJ, Seward JB, Guiliani ER: Echocardiographic assessment of left ventricular filling and septal and posterior wall dynamics in idiopathic hypertrophic subaortic stenosis. Circulation. **57**(3), pp. 512-520, 2009D

[13] Rodriguez EK, Hunter WC, Royce MJ, Leppo MK, Douglas AS: A method to reconstruct myocardial sarcomere lengths and orientations at transmural sites in beating canine hearts. Am J Physiol Heart Circ Physiol. **263**(1), pp. 293-306, 1992D

[14] Sabbah HN, Stein PD: Pressure-diameter relations during early diastole in dogs. Incompatibility with the concept of passive left ventricular filling. Circ Res. **48**(3), pp. 357-365, 1981D

[15] Yun KL, Niczyporuk MA, Daughters GT, Ingeks NB, Stinson EB, Alderman EL, Hansen DE, Miller DC: Alterations in left ventricular diastolic twist mechanics during acute human cardiac allograft rejection. Circulation. **83**(3), pp. 962-973, 1991D

[16] Utaki H, Taniguchi K, Konishi H, Himeno Y, Amano A: A Method for Determining Scale Parameters in a Hemodynamic model incorporating Cardiac Cellular Contraction model. Adv Biomed Eng., 2015.